

Environmental and geographic relationships among salmon forage assemblages along the continental shelf of the California Current

Whitney R. Friedman^{1,2,*}, Jarrod A. Santora³, Isaac D. Schroeder^{1,4}, David D. Huff⁵, Richard D. Brodeur⁶, John C. Field², Brian K. Wells²

¹Institute of Marine Science, University of California, Santa Cruz, 100 McAllister Way, Santa Cruz, CA 95060, USA

²Fisheries Ecology Division, Southwest Fisheries Science Center, National Marine Fisheries Service, National Oceanic and Atmospheric Administration, 110 McAllister Way, Santa Cruz, CA 95060, USA

³Center for Stock Assessment Research, Department of Applied Mathematics and Statistics, University of California, Santa Cruz, 1156 High Street, Santa Cruz, CA 95064, USA

⁴Environmental Research Division, Southwest Fisheries Science Center, National Marine Fisheries Service, National Oceanic and Atmospheric Administration, 99 Pacific Street, Suite 255A, Monterey, CA 93940, USA

⁵Ocean and Estuary Ecology Program, Fish Ecology Division, Northwest Fisheries Science Center, National Oceanic and Atmospheric Administration, 520 Heceta Place, Hammond, OR 97121, USA

⁶Fish Ecology Division, Northwest Fisheries Science Center, National Oceanic and Atmospheric Administration, 2030 S.E. OSU Drive, Newport, OR 97365, USA

ABSTRACT: Ocean entry for salmon (*Oncorhynchus* spp.) is a critical period during which recruitment to the adult population is likely set. During this period, predation risk will be modulated by availability of suitable prey at the time and location of out-migration. Therefore, identifying variables affecting the distribution of prey coast-wide facilitates ecosystem-based management of Chinook salmon *O. tshawytscha* in the California Current. In this study, we quantified distributions of salmon forage assemblages relative to biogeographic breaks and ocean conditions along the California Current shelf ecosystem from Monterey Bay, California (36.5° N), to Willapa Bay, Washington (46.5° N). Epipelagic micronekton samples were collected during late springs of 2011, 2013, 2014, and 2015. We characterized (1) abundance of salmon forage taxa north and south of geographic boundaries, (2) spatial gradients in forage assemblages, and (3) relationships between environment and spatiotemporal variability of forage assemblages. We found higher abundances of market squid *Doryteuthis opalescens*, rockfishes (*Sebastes* spp.), and sanddabs (*Citharichthys* spp.) south of Cape Mendocino, while pandalid shrimp (*Pandalus* spp.), rex sole *Glyptocephalus zachirus*, and smelt (Osmeridae) were more abundant in the north. Multivariate analyses demonstrated a latitudinal gradient in the relative contribution (rank order) of individual taxa to salmon forage assemblages, and further analyses revealed the presence of 4 distinct multi-species assemblages associated with regional and meso-scale oceanographic dynamics. Our findings indicate that distributions of salmon forage assemblages and the oceanographic characteristics associated with those assemblages is similar to the spatial coherence of Chinook salmon population survival observed over longer time series.

KEY WORDS: Biogeography · Ecosystem oceanography · Forage fishes · Salmon · Spatial ecology · California Current

Resale or republication not permitted without written consent of the publisher

INTRODUCTION

Recruitment of Chinook salmon *Oncorhynchus tshawytscha* to the adult population is widely thought to be set during the first few months at sea

(Beamish & Mahnken 2001, Kilduff et al. 2014, Woodson & Litvin 2015, Wells et al. 2016). Previous studies have demonstrated that the initial period at sea is associated with peaks in rates of energy accumulation and growth for juvenile Chinook salmon

(MacFarlane 2010), and availability of appropriate forage on the coastal shelf is associated with increased survival of the out-migrating juveniles (Wells et al. 2012, 2016). When the forage assemblage for out-migrating salmon juveniles is restricted in abundance and/or biomass due to reduced coastal production or is spatially disjointed from out-migrating salmon, juvenile survival can be very low (Brodeur et al. 1992, Wells et al. 2016). Mechanistically, reduced availability of forage results in decreased size and growth of juvenile salmon (Brodeur et al. 1992), which in turn leads to an increased probability of being preyed upon (Woodson et al. 2013, Tucker et al. 2016). Further, population survival estimates of Chinook salmon out-migrating to the northern California Current Ecosystem (CCE) covary with one another significantly more than with those salmon populations out-migrating south (Kilduff et al. 2014). This is likely a result of the spatial coherence of winter downwelling and upwelling dynamics (Parrish et al. 1981, Mueter et al. 2002, Checkley & Barth 2009) demarcated by coastal promontories and known biogeographic breaks in marine fauna (e.g. Cape Mendocino; King et al. 2011, Fenberg et al. 2015, Gottscho 2016). It is therefore of interest, especially for understanding the effects of regional environmental variability on Chinook salmon populations, to discern whether juvenile salmon forage assemblages show a similar pattern of spatial coherence. Moreover, the directed effort toward ecosystem-based fishery management (Pacific Fisheries Management Council 2013), and the development of ecosystem models to inform such efforts (e.g. Ruzicka et al. 2012, Kaplan et al. 2013, Fiechter et al. 2015, Koehn et al. 2016), benefit from an improved understanding of variability in salmon forage assemblages relative to regional and temporal variations in hydrographic processes.

Relationships between environmental determinants affecting forage productivity have been identified and should be considered when assessing variability of salmon forage assemblages and their distribution along the CCE shelf (Wells et al. 2016). Reduced downwelling and increased upwelling in winter promotes availability of nutrients near or at the surface, equator-ward transport of subarctic water, and production of forage on the shelf during winter (Logerwell et al. 2003, Wells et al. 2012, Daly et al. 2013, 2017, Thayer et al. 2014). Specifically, for some salmon forage species, such as young-of-the-year (YOY) rockfishes (*Sebastes* spp.) and sanddabs (*Cithrichthys* spp.), spawning occurs during winter, and the influx of subarctic water masses (Ralston et al. 2013, 2015) and/or nutrients (Schroeder et al.

2014) is positively related to their abundance on the shelf. As spring approaches and the transition to more intense, regular upwelling occurs, the strength and duration of the upwelling season depends, in part, on the date of that transition, as determined by regional winds (Bograd et al. 2009, Schroeder et al. 2013). The transition to the upwelling season is positively related to latitude, such that more northern regions of the CCE initiate upwelling later and experience a shorter upwelling period (Bograd et al. 2009, Black et al. 2011). When the CCE shelf experiences more intense and earlier upwelling relative to the latitude, continued nutrient introduction enables development and maintenance of populations of krill and forage fishes in late spring (Parrish et al. 1981, Schroeder et al. 2014, Wells et al. 2016). These prey populations overlap temporally and spatially with ocean out-migration timing for many Chinook salmon populations (Daly et al. 2013, 2017). However, if upwelling and associated transport is too intense, primary productivity (Garcia-Reyes et al. 2014, Jacox et al. 2015) and prey (Cury & Roy 1989, Santora et al. 2011, Ralston et al. 2013) can be advected off the shelf, making them unavailable to juvenile salmon. Ultimately, the overlap in timing of out-migration and the development and retention of a forage base on the shelf is key to ensuring that the energetic needs of juvenile out-migrants are met (e.g. Logerwell et al. 2003, Wells et al. 2012, Satterthwaite et al. 2014).

Based on the current understanding of CCE dynamics, the conceptual model that underlies our study is that the survival of juvenile salmon is related to the availability of prey on the shelf during the first few months at sea, and that the composition and abundance of forage assemblages on which salmon rely is ultimately determined by winter regional-scale (e.g. upwelling; 100–1000 km) and spring meso-scale (e.g. retentive regions, Wing et al. 1998; 10–100 km) hydrographic processes (Checkley & Barth 2009, Wells et al. 2016, Riddell et al. 2018). Along the CCE, when juvenile Chinook salmon out-migrate to sea, they mostly rely on juvenile fishes, amphipods, decapods, and euphausiids (hereafter krill) as important prey resources (Brodeur et al. 2007, Wells et al. 2012, 2016). As juvenile salmon grow, they broaden their diet to include progressively larger juvenile fishes and other prey when available (Daly et al. 2009). However, the diets of juvenile Chinook salmon vary along the CCE (Brodeur et al. 2007, Hertz et al. 2015), with differences likely attributable to variability in forage assemblages (Brodeur et al. 2007) resulting from spatiotemporal environmental variability (Brodeur & Pearcy 1992, Wells et al. 2012, 2016). These differ-

ences in diet show within-region coherence in composition (Hertz et al. 2015), suggesting a regional coherence of available forage assemblages.

We evaluated the relationships between spatio-temporal variability of ocean conditions and the composition of forage assemblages used by juvenile Chinook salmon over a large region of the CCE shelf (36.5–46.5°N). We hypothesized that the distributions of distinct salmon forage assemblages relate to biogeographic boundaries (i.e. capes, see Fenberg et al. 2015) and environmental dynamics associated with those boundaries (e.g. upwelling characteristics) along the CCE. We focused on epipelagic micro-nekton species known to occur in juvenile salmon diets and sampled in regions overlapping with juvenile salmon distributions. Based on our conceptual model of the system, we related these samples to upwelling dynamics in winter, and water mass and transport dynamics in spring and early summer. Throughout the CCE, physical forcing patterns and forage assemblage structure tend to exhibit their largest gradients at the large coastal promontories, such as Cape Blanco and Cape Mendocino (Fig. 1; Checkley & Barth 2009, Phillips et al. 2009, Fenberg et al. 2015, Gottscho 2016). Therefore, we hypothesized that a similar boundary at coastal promontories may exist in the salmon forage assemblage in the northern-central CCE.

MATERIALS AND METHODS

Collection of epipelagic micronekton

Epipelagic micronekton samples were collected during May and June by the Southwest Fisheries Science Center Rockfish Recruitment and Ecosystem Assessment Survey and the Northwest Fisheries Science Center Pre-recruit Groundfish Survey. Data were extracted for the region from Monterey Bay, California (36.5°N) to Willapa Bay in southern Washington (46.5°N). A modified midwater Cobb trawl (30 m headrope depth where bottom depth was >50 m, 10 m headrope where bottom depth was <50 m) was towed for 15 min at 2 knots (distance of ~1 km) during hours of darkness to collect epipelagic species along the CCE in the mixed layer where juvenile salmon are typically found (Sakuma et al. 2016). Methods were standardized between regions beginning in 2011. To match the habitat distribution of juvenile Chinook salmon (Bi et al. 2011, Hassrick et al. 2016), we restricted samples analyzed to data from trawls conducted where bottom depth was

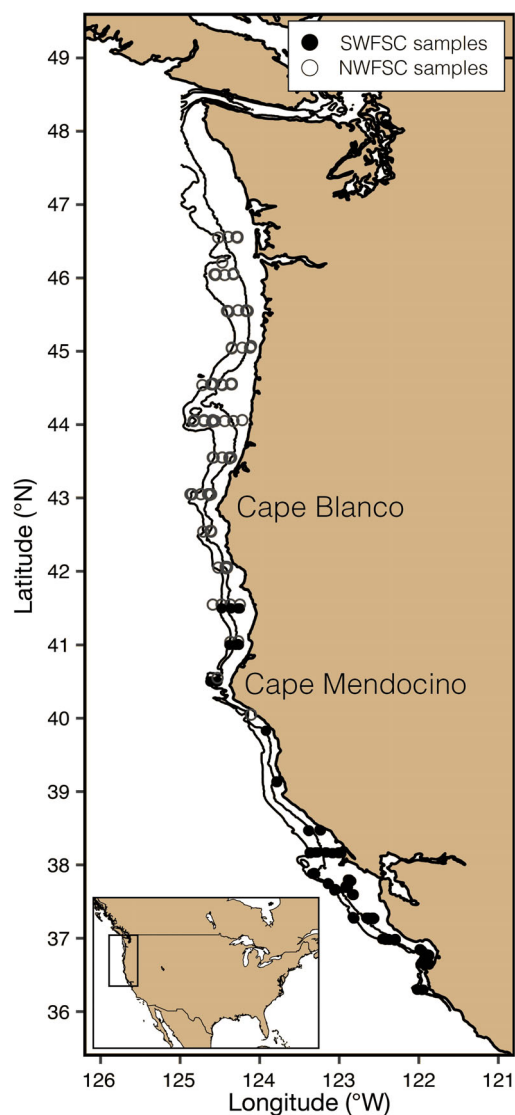


Fig. 1. Distribution of the 297 trawls in depths ≤ 200 m that were used in the analyses. Samples were collected by the Northwest Fisheries Science Center (open circles, NWFSC) and Southwest Fisheries Science Center (filled circles; SWFSC) of the National Marine Fisheries Service during May and June 2011, 2013, 2014, and 2015. Isobaths shown are at 100 and 200 m

≤ 200 m. In total, we used 297 trawls collected across 72 fixed stations (Fig. 1), covering the years 2011, 2013, 2014, and 2015 (trawls were not conducted across the complete study range in 2012). Of the 297 trawls used, 196 were collected south of Cape Mendocino (40.5°N), and 34 samples were within-year repeats. The median days apart for those sampled twice within a year ($n = 28$) was 10.5 d, and 16 d for those sampled 3 times within a year ($n = 6$). Repeat within-year samples were controlled for in the analyses.

We restricted our analysis of epipelagic micronekton sampled to those of appropriate size to be eaten by out-migrating salmon (including only YOY life stages where appropriate) (Daly et al. 2009); the final selection of taxa represented a size range (standard length) of 13.0–69.0 mm (mean = 37.72 mm). Species were grouped into the lowest identified taxonomic groups. To reduce the influence of very rare species, only taxa that were present in at least 1% of the 297 trawls were used in the analysis (Table 1). Of the 31 taxa analyzed in this study, all but 1, combfish (Zaniolepididae), are confirmed prey of juvenile Chinook salmon based on stomach content analyses (Brodeur 1989, Brodeur & Pearcy 1990, MacFarlane & Norton 2002, Schabetsberger et al. 2003, Brodeur et al. 2007, 2011, Daly et al. 2009, 2010, Wells et al. 2012, E. Daly

unpubl. data). Total krill abundance (primarily *Euphausia pacifica* and *Thysanoessa spinifera*; Santora et al. 2012a) was measured from the same trawls; however, we quantified the abundance and geographic distribution of krill separately due to the ubiquity and overall greater abundance of krill along the CCE (Santora et al. 2012b, Dorman et al. 2015).

Oceanographic data

Environmental variables used in our assessment of salmon forage assemblages were chosen *a priori* based on published relationships between the dynamics of the CCE and development of the forage assemblage on the shelf (Table 2; Hickey 1979, Loger-

Table 1. Epipelagic micronekton taxa representing salmon forage considered in our analyses (Brodeur 1989, Brodeur & Pearcy 1990, MacFarlane & Norton 2002, Schabetsberger et al. 2003, Brodeur et al. 2007, 2011, Daly et al. 2009, 2010, Wells et al. 2012, E. Daly unpubl. data). Non-metric multidimensional scaling (NMS) axis 1 and axis 3 scores (abundance weighted centroids of site scores for which the taxon was observed) are presented for each of the 30 taxa included in the NMS analysis, as well as the significance of their relationship to the ordination space (* $p < 0.05$). Within-assemblage ranked abundances show the relative contribution of each taxon to the assemblages (A1–A4) identified by the regression-tree analysis (Fig. 3). Bold values indicate the top 5 ranked taxa for each assemblage type. Assemblages A1–A4 are consistent with Table 3 and Figs. 3 & 4

No.	Common name	Taxon	Axis scores & significance			Within-assemblage ranks			
			Axis 1	Axis 3	p	A1	A2	A3	A4
1	Armhook squid	<i>Gonatus</i> spp.	0.204	−0.979	0.061	8	5	7	13
2	Arrowtooth flounder	<i>Atheresthes stomias</i>	−0.646	−0.764	0.601	9	20	4	23
3	Barracudina	Paralepididae	0.493	−0.870	0.159	–	–	–	27
4	Blacktip squid	<i>Abraliopsis felis</i>	0.114	−0.993	0.042*	14	15	14	22
5	Combfish	Zaniolepididae	0.753	0.658	0.089	–	13	–	18
6	Dover sole	<i>Microstomus pacificus</i>	0.749	−0.663	0.087	21	18	12	20
7	Lingcod	<i>Ophiodon elongatus</i>	0.733	0.680	0.026*	–	–	–	7
8	Market squid	<i>Doryteuthis opalescens</i>	0.741	0.671	<0.001*	15	4	11	1
9	Myctophids	Myctophidae	−0.174	−0.985	0.044*	12	12	12	11
10	Northern anchovy	<i>Engraulis mordax</i>	0.546	0.838	0.01*	–	21	–	8
11	Octopus	Octopoda	0.557	−0.831	0.02*	20	9	14	12
12	Pacific hake	<i>Merluccius productus</i>	0.424	−0.906	0.002*	13	11	5	5
13	Pacific sand lance	<i>Ammodytes hexapterus</i>	−0.718	−0.696	0.009*	17	–	–	29
14	Pacific sardine	<i>Sardinops sagax</i>	0.614	0.789	0.19	–	–	–	14
15	Pacific tomcod	<i>Microgadus proximus</i>	−0.994	0.110	0.139	18	17	14	29
16	Painted greenling	<i>Oxylebius pictus</i>	0.937	0.350	0.059	–	–	–	25
17	Pandalus shrimp	<i>Pandalus jordani</i>	−0.583	−0.812	0.829	1	2	1	4
18	Poacher	Agonidae	−0.341	−0.940	0.511	22	22	14	28
19	Rex sole	<i>Glyptocephalus zachirus</i>	0.410	−0.912	0.04*	6	6	8	9
20	Rockfish	<i>Sebastes</i> spp.	0.996	−0.086	<0.001*	4	1	3	2
21	Ronquil / prickleback	<i>Ronquilus</i> / Stichaeidae	0.355	0.935	0.758	11	22	9	15
22	Sand sole	<i>Psettichthys melanostictus</i>	−0.070	0.998	0.185	7	7	6	10
23	Sanddab	<i>Citharichthys</i> spp.	0.848	−0.531	<0.001*	5	3	2	3
24	Sculpin	Cottidae	0.998	0.068	0.003*	19	16	–	16
25	Sergestid	Sergestidae	−0.053	−0.999	0.007*	2	19	–	19
26	Shrimp	Natantia	0.872	0.490	0.134	–	–	–	26
27	Slender sole	<i>Lyopsetta exilis</i>	0.434	−0.901	0.014*	10	10	10	6
28	Smelt	Osmeridae	−0.745	−0.667	0.443	3	8	–	17
29	Snailfish	Liparidae	−0.521	−0.854	0.036*	16	–	14	24
30	Turbot	<i>Pleuronichthys</i> spp.	0.995	−0.102	<0.001*	22	14	–	21
31	Krill	Euphausiidae	–	–	–	–	–	–	–

Table 2. Environmental variables used to assess the distribution of salmon forage assemblages. Conceptually, these variables were chosen to examine the influence of winter preconditioning, water mass characteristics, and transport on the distribution of juvenile salmon forage assemblages

Variable	Definition	Influence
Regional abundance of forage		
UI_{t-4}	Coastal upwelling index 4 months prior to sample date	Reduced downwelling and upwelling in winter represents preconditioning of the system by reducing stratification and promoting nutrient availability onto the shelf early in the season
$d26_{t-4}$	Depth of the 26.0 kg m^{-3} isopycnal 4 months prior to sample date	Represents availability of nutrients to the surface. A shallow 26.0 kg m^{-3} isopycnal in the winter has been associated with increased production of phytoplankton and forage species on the shelf
Mesoscale distribution of forage		
U_{t-0}	Meridional (East, West) components of water velocity at 20–40 m during the month of the trawl. Positive values of U are eastward	Surface currents relate to the advection and retention of larval and juvenile fish on the shelf, and transport of organisms between regions
V_{t-0}	Zonal (North, South) components of water velocity at 20–40 m during the month of the trawl. Positive values of V are northward	
$Temp_{t-0}$	Temperature at 20–40 m during the month of the trawl	Identifies water masses that can entrain forage species

well et al. 2003, Checkley & Barth 2009, Schroeder et al. 2014, Wells et al. 2016). Reduced downwelling and upwelling in winter represent preconditioning of the system by reducing stratification and promoting nutrient availability on the shelf early in the season (Logerwell et al. 2003, Schroeder et al. 2009). The depth of the 26.0 kg m^{-3} isopycnal during winter represents availability of nutrients to the surface layer. A shallow 26.0 kg m^{-3} isopycnal in the winter has been associated with increased production of phytoplankton (Jacox et al. 2016) and forage species on the shelf (e.g. juvenile rockfishes and krill; Schroeder et al. 2014). Eastward and northward surface currents during spring relate to the advection and retention of larval and juvenile fishes on the shelf, and transport of organisms between regions (Bakun & Parrish 1982, 1990, Cury & Roy 1989, Largier et al. 2006, Dorman et al. 2011). Spring temperatures and salinities at the depth of the trawl samples are representative of particular water masses that may indicate forage species associations and their spatial distribution (Largier et al. 2006, Santora et al. 2012b). Here, we focus only on temperature, as salinity was highly correlated to temperature at the scale we examined (i.e. salinity was removed from models to avoid collinearity issues).

Modeled oceanographic data at the time and location of each trawl, as well as at 4 mo prior to each trawl (to assess preconditioning effects following results from Logerwell et al. 2003, Schroeder et al.

2009) were derived from a data-assimilative regional ocean modeling system (ROMS; Moore et al. 2011). Variables derived from ROMS (spatial resolution 10 km) included: depth of 26.0 kg m^{-3} isopycnal 4 mo prior to each trawl (Table 2, $d26_{t-4}$), temperature at 20–40 m during the month of the trawl (Table 2, $Temp_{t-0}$), as well as meridional and zonal components of water velocity at 20–40 m during the month of the trawl (Table 2, U_{t-0} and V_{t-0} , respectively). The depth of 20–40 m was selected because it matched the target depth for trawl samples (Sakuma et al. 2016). For each trawl, we calculated values for each ROMS variable by averaging all ROMS data points over a radius of 56 km from the starting latitude and longitude and month of the sample. We could not justify a higher resolution of environmental data given likely transport dynamics occurring through the months, nor could we justify restricting the environmental data to a shorter time frame given relatively high variability in oceanographic conditions during the preconditioning and upwelling seasons.

The coastal upwelling index has been used extensively to estimate coastal upwelling in the CCE (Bakun 1973, Bograd et al. 2009). The upwelling index is calculated from the cross-shelf component of Ekman mass transport (Schwing et al. 1996) and can be calculated from meridional and zonal components of the wind stress vector that are rotated by the coastal angle to resolve the normal component to the

shore line. We downloaded monthly means of Ekman transport vectors (1° spatial resolution) from NOAA's west coast regional node of CoastWatch (<http://coastwatch.pfeg.noaa.gov/erddap/griddap/erdlasFnWPr.html>), rotated the vectors by the coastal angle, and then divided the resultant Ekman transport by -10 to put the values in units of $\text{m}^3 \text{s}^{-1} 100 \text{ m}^{-1}$ of coastline, which is consistent with units used to represent upwelling intensity. This resulted in negative values indicating downwelling and positive values indicating upwelling. We used linear interpolation (implemented in Python 2.7.13, using the function 'griddata', method 'linear' in the package 'SciPy'; Jones et al. 2001) to create a spatially interpolated surface of Ekman transport values and extracted the interpolated values at the start location of each trawl 4 mo prior to sampling (Table 2, UI_{t-4}).

Oceanographic conditions along CCE during years investigated

We examined catch rates of epipelagic micronekton collected during late spring of 2011, 2013, 2014, and 2015. These years had coast-wide coverage using consistent sampling methods, and represent a broad range of environmental conditions. These environmentally divergent years allowed for a natural experiment to parse general rules governing salmon forage assemblages along the CCE from year-specific conditional drivers. In winter 2011, weak upwelling and occasional downwelling dominated the central CCE and downwelling dominated in the northern CCE, a condition typical of the northern CCE but a negative upwelling anomaly for the central CCE (Bjorkstedt et al. 2012). Winter conditions in 2013 were characterized by a lack of downwelling and occasional upwelling in the northern CCE and stronger than typical upwelling in the central CCE, with positive upwelling anomalies along the central to northern CCE (Wells et al. 2013). In 2014 and 2015, sea surface temperatures were observed to be anomalously high in nearly all regions of the Northeast Pacific (Leising et al. 2015, Di Lorenzo & Mantua 2016, Sakuma et al. 2016). As well, during winter transitioning from 2013 to 2014, basin-scale indicators (i.e. Pacific Decadal Oscillation, Multivariate El Niño Southern Oscillation Index, and North Pacific Gyre Oscillation; Mantua et al. 1997, Wolter & Timlin 1998, Di Lorenzo et al. 2008, respectively) switched phase, indicating less productive conditions and a looming El Niño (Leising et al. 2014, 2015) that ultimately initiated in 2015/2016 (McClatchie et al.

2016). Despite these larger basin-scale patterns, temperatures in both 2014 and 2015 remained relatively cool nearshore into late spring during our sampling period (McClatchie et al. 2016), and the abundance of many forage species (particularly YOY rockfish and YOY sanddabs) was high (Sakuma et al. 2016). Winter upwelling was typical in 2014 but slightly weaker in 2015 (Leising et al. 2015). During 2015, the depth of the 26.0 kg m^{-3} isopycnal during winter, which shoals during upwelling and represents availability of nutrients to the surface, was depressed (Jacox et al. 2016).

Characterizing forage assemblages

We used univariate and multivariate analyses to evaluate the likelihood of spatial and temporal differences in salmon forage assemblages within the CCE. For the univariate analysis, samples were binned by the latitude at which they were collected north (101 trawls) or south (196 trawls) of 40.5° N (Cape Mendocino). We described mean differences in catch per unit effort (CPUE; number observed per trawl) of individual taxa north and south of Cape Mendocino. We used non-metric multidimensional scaling (NMS) to resolve gradients in salmon forage assemblages among the 297 trawls (all years combined) (McCune et al. 2002). NMS analysis was implemented in Program R (v3.2.3; R Core Team 2015) using the package 'vegan' (Oksanen et al. 2016). CPUE data were square-root transformed prior to analysis to reduce the influence of highly abundant species and individual large catches. Dissimilarities between sample units (trawls) were calculated using the Bray-Curtis (Sørensen) measure (Bray & Curtis 1957, McCune et al. 2002). Analysis of the stress statistic indicated that 3 axes were appropriate for this dataset (final stress < 15). NMS plots were rotated so that the greatest variation in the data was represented by axis 1.

Taxa were fit onto NMS space by performing a linear regression of the form

$$y = \beta_1 X_1 + \beta_2 X_2 + \varepsilon \quad (1)$$

where y represents a vector of CPUE data for each taxon, X_1 are the NMS scores on one axis and X_2 are the NMS on a second axis. The observed R^2 value for the linear regression was compared against 10 000 random permutations of the taxon CPUE vector. The resulting p-values represent the proportion of times a randomized R^2 from the distribution was equal to or greater than the observed R^2 value ('vegan' function 'envfit', Oksanen et al. 2016). To visualize taxonomic

indicators of assemblages, taxa significantly related to NMS space ($p < 0.05$) were presented with vectors showing the direction of the relationship, and vector length corresponded to the strength of the correlation.

Evaluating environmental determinants of forage assemblages

To determine whether distinct assemblages were associated with environmental conditions, the resulting NMS axis scores were used as the numerical response variables in a regression tree analysis (Breiman et al. 1984, De'ath & Fabricius 2000, Fenberg et al. 2015). Regression tree analysis is a non-parametric decision-tree machine learning technique used to predict the response of a dependent variable based on several, possibly interacting, input variables. It works by recursively splitting a dataset based on the best value among the set of predictor variables that produces 2 maximally homogenous groups. Our analysis was implemented in Program R using the package 'rpart' (Therneau et al. 2015) to model the distribution of each of the 3 NMS axis scores (our response variables) based on the oceanographic conditions we associated with each trawl (Table 2). Resulting trees were pruned to minimize misclassification error and model complexity, based on the results of 10-fold cross-validation (Breiman et al. 1984, Therneau & Atkinson 1997, 2018, De'ath & Fabricius 2000, Loh 2011). Each axis was modeled separately. Based on the conceptual model defined above, the explanatory variables we tested were upwelling index during the fourth month preceding each trawl (UI_{t-4}), depth of the 26.0 kg m⁻³ isopycnal during the fourth month preceding each trawl ($d26_{t-4}$), temperature during the month of the trawl ($Temp_{t-0}$), and meridional and zonal components of surface velocity during the month of the trawl (U_{t-0} and V_{t-0} , respectively) (Table 2). Pairwise correlation coefficients (Pearson's r) among co-variates included in the analysis ranged from 0.07–0.61, and the maximum observed variance inflation factor was 2.18, each below established threshold values for collinearity (Dormann et al. 2013).

Krill analysis

Given that krill are ubiquitous in the study region (Santora et al. 2012b, Dormann et al. 2015) and are a particularly important component of salmon diet (Wells et al. 2012), we chose to examine how the

same set of environmental variables influenced krill distribution and abundance. Generalized additive models (GAMs) were used to assess the distribution and abundance of krill relative to the same 5 oceanographic variables used in the previous analysis and latitude (R package 'mgcv,' function 'gam;' Wood 2006). GAMs were used rather than linear models as we did not assume a linear relationship between krill abundance and co-variates. Total krill abundance in each trawl (all species) was summed and log-transformed [$\ln(\text{Krill CPUE}+1)$]. We included a random effect of *Station-Year* to account for stations that were re-sampled within a year, and tested whether a random effect of *Year* was required to account for residual spatial autocorrelation in the final model. GAMs were constructed with a Gaussian distribution and identity link function. The full model was specified as

$$\begin{aligned} \ln(\text{Krill CPUE}+1) = & s_1(UI_{t-4}) + s_2(d26_{t-4}) + s_3(Temp_{t-0}) \\ & + s_4(U_{t-0}) + s_5(V_{t-0}) + s_6(\text{Station-Year}, \text{re}) \\ & + s_7(\text{Year}, \text{re}) \end{aligned} \quad (2)$$

For this model, s are cubic smoothing splines with up to 10 knots, and the term 're' indicates random effects. Akaike's information criterion (AIC) (Sakamoto et al. 1986) was used to select the best model among candidate solutions. All models within an AIC difference (Δ) of < 2 are reported (Burnham & Anderson 2003), as well as adjusted R-squared and deviance explained (Wood 2006).

RESULTS

Characterization of salmon forage assemblages

The univariate analysis comparing abundances of each taxon north and south of Cape Mendocino revealed differences between the regions (Fig. 2A). Central CCE samples ($< 40.5^\circ \text{N}$) included higher abundances of market squid *Doryteuthis opalescens*, YOY rockfishes, and YOY sanddabs. Northern trawls tended to include higher abundances of pandalid shrimp (*Pandalus* spp.), rex sole *Glyptocephalus zachirus*, and smelt (Osmeridae). Of these, rockfishes, sanddabs, and smelts are common salmon prey items (see citations in Table 1).

NMS analysis resolved gradients in the relative contributions of taxa collected in each trawl sample. Three dimensions were sufficient to explain most of the variability in the observed forage assemblages (stress = 14.8%). The proportion of variance represented by the 3 axes between the original distance

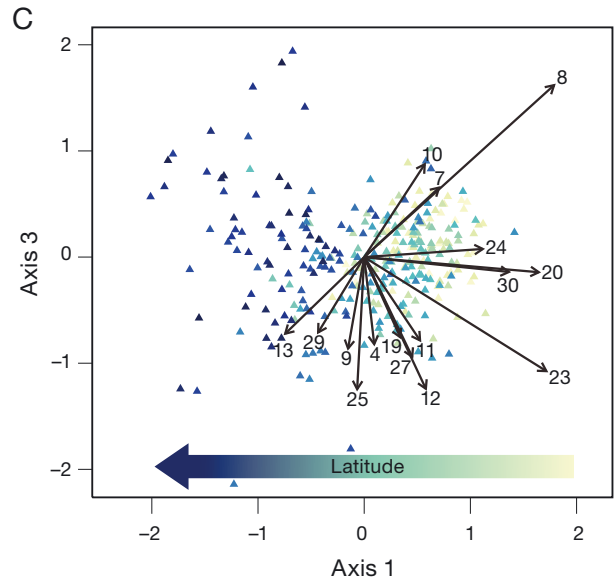
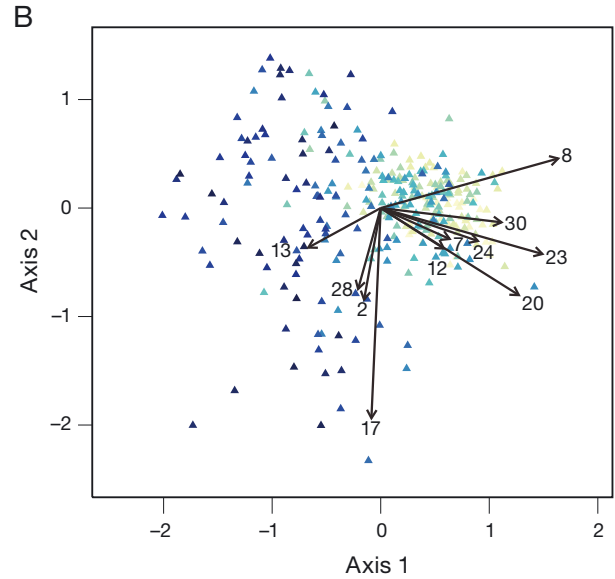
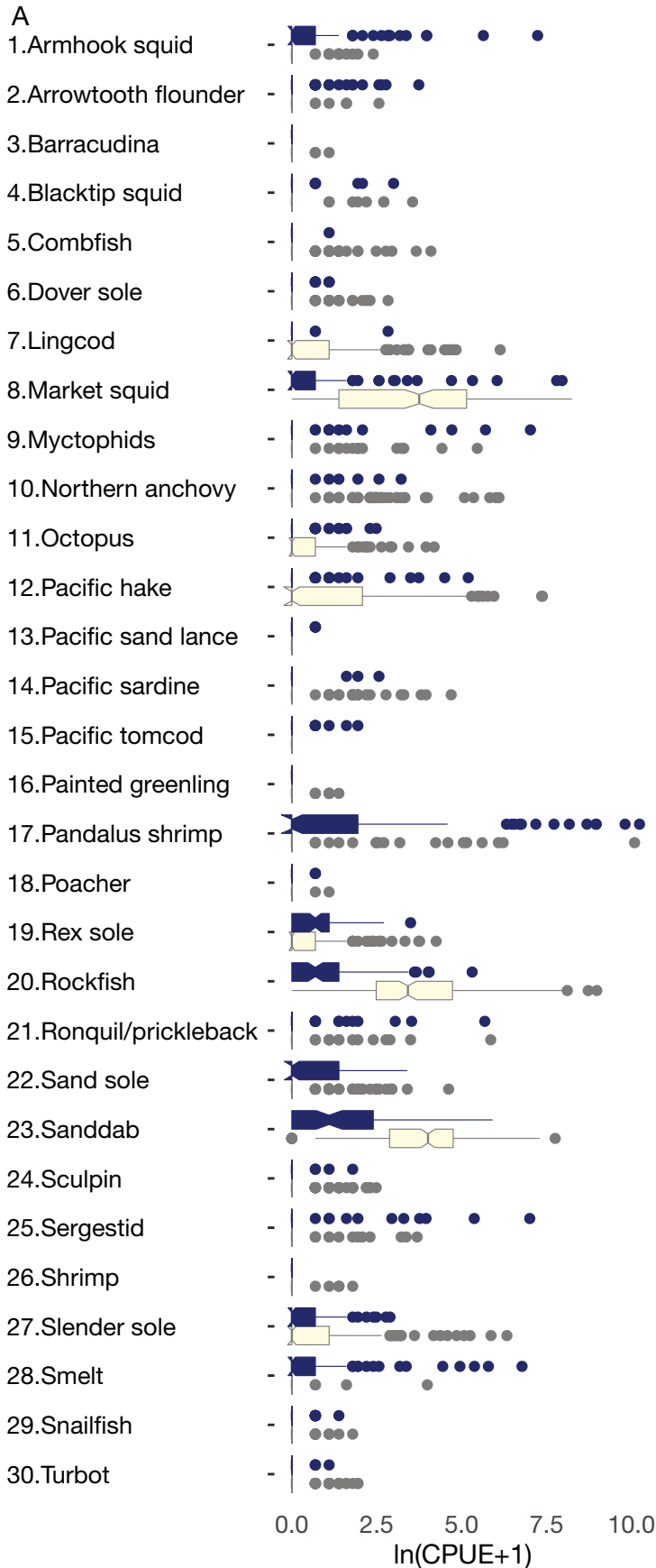


Fig. 2. (A) Abundances of the 30 taxa examined in this study (Table 1) north (blue) and south (yellow and grey) of Cape Mendocino (40.5° N). Notches represent 95% confidence intervals around the median; non-overlapping notches indicate strong evidence for a difference in medians (Chambers et al. 1983). Whiskers represent values within 1.5*IQR (inter-quartile range) of the upper and lower quartiles. CPUE: catch per unit effort. (B,C) Results from the non-metric multidimensional scaling (NMS) ordination of forage assemblages caught in 297 trawls. Variability in axis 1 is associated with latitude as indicated by the color gradient from low latitudes (min = 36.3° N, yellow) to high latitudes (max = 46.5° N, dark blue). (B) Ordination results for axis 1 and 2. Taxa significantly related to NMS space ($p < 0.05$) are presented with vectors showing the direction of the relationship and vector length corresponds to the strength of the correlation. Numbers represent taxa as listed in panel A and Table 1. (C) Ordination results for axes 1 and 3. Statistics for taxa significantly related to NMS space are shown in Table 1

matrix and the ordination distances was $R^2 = 0.90$ (Fig. 2B,C). Axis 2 represents the rare samples containing large collections of pandalid shrimp relative to other taxa (Fig. 2B). We focus our NMS results on the relationships uncovered by axes 1 and 3 because they represent spatial characteristics of salmon forage assemblages.

Of the 30 taxa, 16 were significantly correlated with the first and third dimensions of the NMS ordination (Table 1, Fig. 2C). NMS axis 1 scores were negatively related to the latitude at which the sample was collected, and therefore represent the presence of a latitudinal gradient in relative contribution (rank order) of taxa to the forage assemblages (Fig. 2B,C). Southern assemblages were characterized by higher relative contributions of market squid, rockfishes, and sanddabs. The relative contribution of Pacific sand lance *Ammodytes hexapterus* was greater in northern assemblages. Pacific sand lance, while rare overall, were present in nearly 10% of samples collected north of 43.5°N and in none south of that. Axis 3 represents variation attributed to species with either on- or more off-shore affinities occurring on the shelf during sampling (as determined by Santora et al. 2012a and Ralston et al. 2015). Those species for which production depends on shelf conditions (greater axis 3 scores) include lingcod *Ophiodon elongatus*, market squid, and YOY northern anchovy *Engraulis mordax*. Off-shelf derived taxa include YOY Pacific hake *Merluccius productus* and sergestids (Sergestidae) (Fig. 2C).

Environmental determinants of forage assemblages

Regression tree analysis revealed assemblages associated with spatiotemporal patterns of winter upwelling (UI_{t-4}), the depth of the 26.0 kg m⁻³ isopycnal in winter ($d26_{t-4}$), and sea temperature during the sampling month ($Temp_{t-0}$). The regression tree model for axis 1 scores (representing latitudinal gradient) resulted in 4 leaves, referred to here as assemblage types ($R^2 = 0.54$, RMSE = 0.48, Fig. 3). The first split was represented by winter upwelling values: 73% of samples were associated with very weak winter downwelling or upwelling ($UI_{t-4} \geq -12 \text{ m}^3 \text{ s}^{-1} 100 \text{ m}^{-1}$, mean = 16.5) and the remaining 27% of samples were associated with stronger winter downwelling ($UI_{t-4} < -12 \text{ m}^3 \text{ s}^{-1} 100 \text{ m}^{-1}$, mean = -49.8; Fig. 3). Secondly, the assemblages associated with winter downwelling (assemblages 1 and 2, purple and blue in Figs. 3 & 4A–H) were differentiated by warmer ($Temp_{t-0} \geq 9.7^\circ\text{C}$, mean = 10.6; 18% of samples) or

cooler ($Temp_{t-0} < 9.7^\circ\text{C}$, mean = 9.4; 9% of samples) sea temperatures during the survey. The samples associated with winter upwelling (assemblages 3 and 4; green and orange in Figs. 3 & 4I–P) were differentiated by shallower ($d26_{t-4} > -106 \text{ m}$, mean = -97.7; 2% of trawls) or deeper ($d26_{t-4} \leq -106 \text{ m}$, mean = -131.8; 71% of samples) 26.0 kg m⁻³ isopycnals 4 mo prior to sampling. Regression tree analyses for NMS axes 2 and 3 scores were uninformative (no splits) and likely represent assemblage characteristics that were associated with environmental drivers unaccounted for in our conceptual model.

Interannual variability

Assemblage types 1 (purple; Fig. 4A–D) and 2 (blue, Fig. 4E–H) were primarily observed north of 40.5°N (Cape Mendocino) during the 4 sampling years; only 3 trawls occurred south of Cape Mendocino. Largely, assemblage type 1 was present in 2011, 2013, and 2014 (90.4% of trawls in that assemblage) and assemblage 2 was almost entirely restricted to 2014 and 2015 (96.4% of trawls in that assemblage; Table 3). The northern assemblages (assemblages 1 and 2) were clearly differentiated by local temperatures (Figs. 3 & 4A–H). For example, a comparison of the distributions in 2014 of assemblage 1 (Fig. 4C) and the distribution of assemblage 2 (Fig. 4G) indicate they do not overlap based on temperatures during sampling. All 4 years show a similar degree of separation, with assemblage 1 associated with temperatures warmer than 9.7°C, and assemblage 2 associated with temperatures cooler than 9.7°C (Figs. 3 & 4A–H). While assemblage type 2 was statistically associated with downwelling and cooler temperatures (Fig. 3), in 2014 it existed in a region of relatively strong upwelling (Fig. 4C,O), indicating that the presence of upwelling is not exclusive of assemblage type 2. Assemblage type 1 had 23 taxa represented, with smelt and sergestids being relatively more abundant than any of the other 3 assemblages (Table 1). Assemblage type 2 had the same number of taxa but these samples had decreased representation of smelt and sergestids, and increased representation of market squid and rockfishes.

Assemblage type 4 (orange) was predominantly a central CCE assemblage through all 4 years; however, in 2013, it had a small representation (4 trawls) north of Cape Blanco as well, possibly due to a lack of typical downwelling in the northern CCE (Fig. 4B,N). Assemblage type 4 was represented by all 30 taxa (Table 1). It was the only assemblage with barracud-

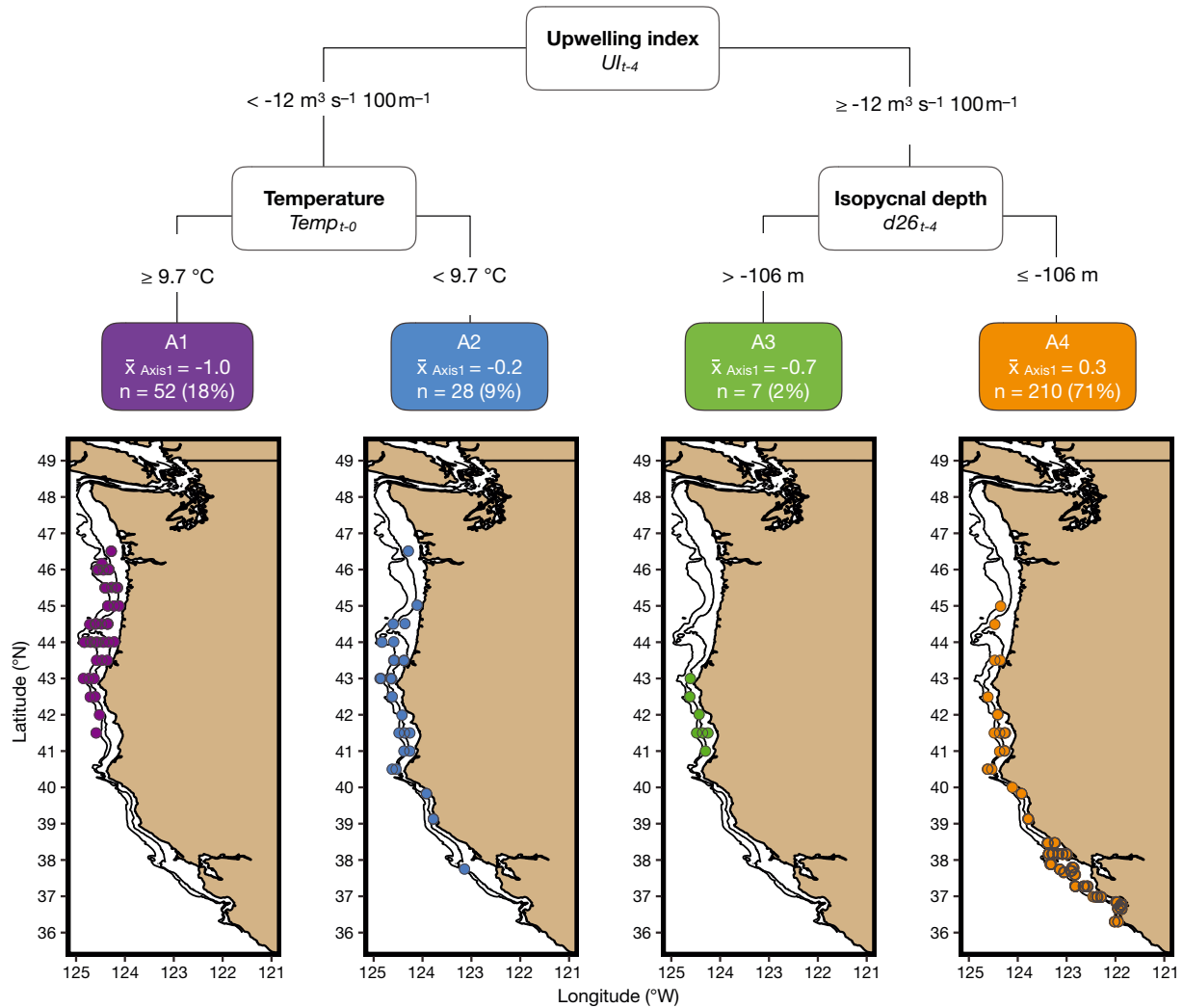


Fig. 3. Four assemblage types (A1–A4) based on regression tree analysis of non-metric multidimensional scaling axis 1 scores. Values in the colored boxes represent mean axis scores and number and percentage of samples allocated to each assemblage type. Maps show individual trawls for each assemblage type. Further detail on these assemblages can be found in Tables 1 & 3

ina (Paralepididae), lingcod, Pacific sardine *Sardinops sagax*, painted greenling *Oxylebius pictus*, or shrimp (Nantantia). Market squid ranked first in this assemblage, higher than in any other assemblage.

Assemblage type 3 had the fewest taxa represented (18 taxa; Table 1) due, in part, to its small representation (7 trawls; Fig. 3). Unlike other assemblages, arrowtooth flounder *Atheresthes stomias* were relatively abundant (Table 1). Assemblage type 3 was only present during 2013 and only in the confined area between Capes Blanco and Mendocino concurrent with a relatively shallow 26.0 kg m^{-3} isopycnal (Fig. 4J). Both assemblages 3 and 4 included higher representations of Pacific hake relative to other taxa.

In sum, there were notable interannual patterns in the presence and distribution of the 4 assemblages.

Assemblage types 1 and 4 were present in all 4 years, and the only ones represented in 2011. Northern assemblage types (1 and 2) occupied different, yet adjacent, water masses defined here by temperature. In 2013, the typically more southern assemblage type (4) spread across the CCE, but was missing from the area between the capes associated with assemblage 3, which was not present in any other sample year.

Krill distribution

Krill were ubiquitous, occurring in 88% of samples. However, relatively more krill were caught in central California than elsewhere on the coast (Fig. 5A). Three models for describing the association of krill abundance relative to environmental conditions

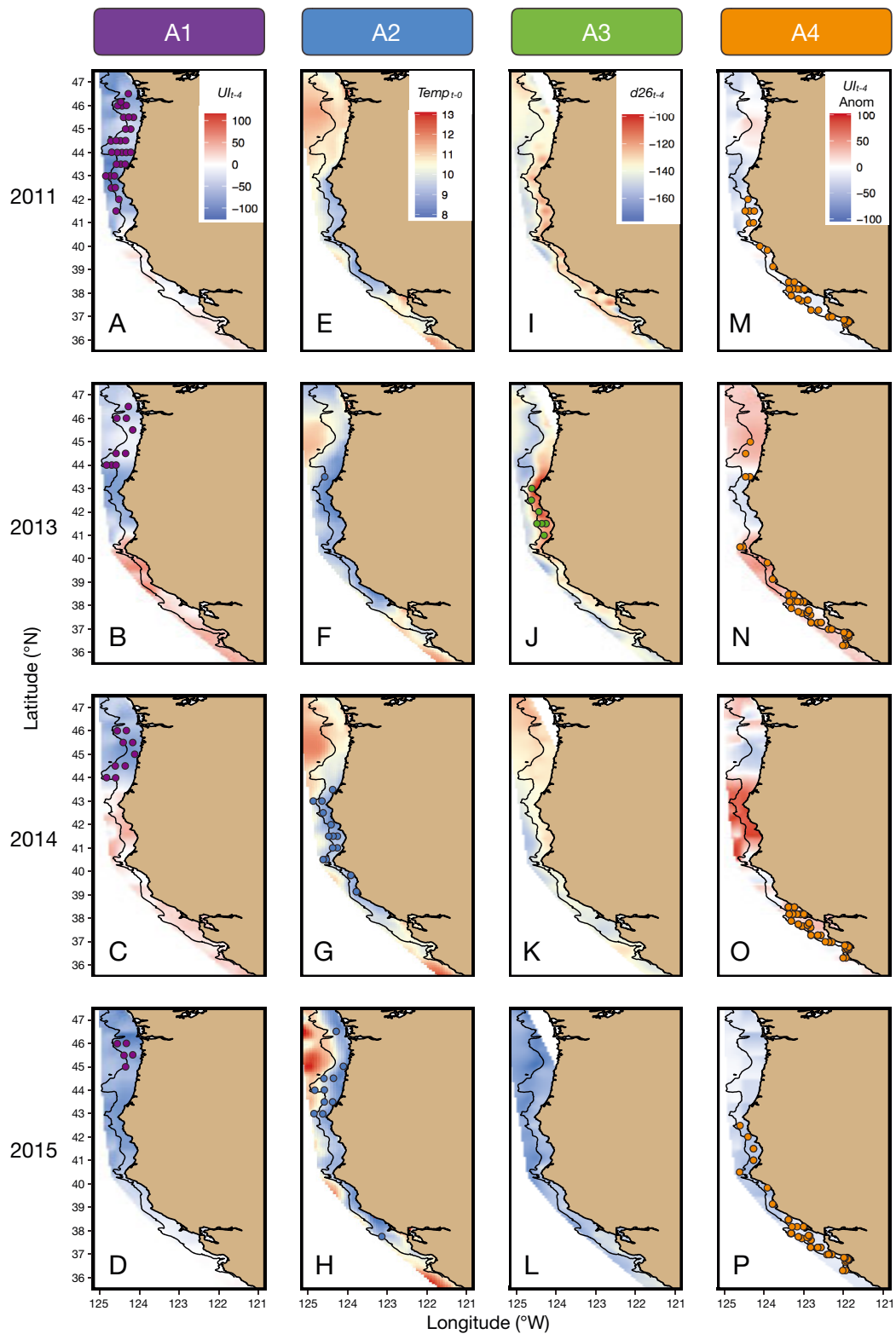


Fig. 4. Annual distributions of 4 salmon forage assemblage types (A1–A4) overlaid on environmental gradients for (A–D) UI_{t-4} , (E–H) $Temp_{t-0}$, (I–L) $d26_{t-4}$, and (M–P) anomalies for UI_{t-4} across the 4 study years (observation – mean); variables are defined in Table 2. UI_{t-4} anomalies are shown to demonstrate interannual variability in regional patterns but were not used in analysis. Due to a shallow depth and substantial freshwater input, the nearshore area within the Columbia River plume (~46°N) did not have isopycnal densities $\geq 26.0 \text{ kg m}^{-3}$ (therefore none are shown). Assemblages A1–A4 are consistent with Tables 1 & 3

were within $\Delta AIC \leq 2$ (Table 4). All top models included temperature during sampling ($Temp_{t-0}$), and depth of the 26.0 kg m⁻³ isopycnal 4 mo prior ($d26_{t-4}$). Additional terms included winter upwelling (UI_{t-4}) and local meridional transport during the time of

Table 3. Four assemblage types (A1–A4) that resulted from the regression tree model for axis 1 (Fig. 3). Columns include number of trawls (n) in each assemblage type during each sampling year and the percentage of total trawls from each assemblage that were observed in each year (% total). Assemblages A1–A4 are consistent with Table 1 and Figs. 3 & 4

	A1		A2		A3		A4	
	n	% total	n	% total	n	% total	n	% total
2011	29	56	0	0	0	0	41	20
2013	9	17	1	4	7	100	56	27
2014	9	17	16	57	0	0	61	29
2015	5	10	11	39	0	0	52	25
Total samples	52		28		7		210	

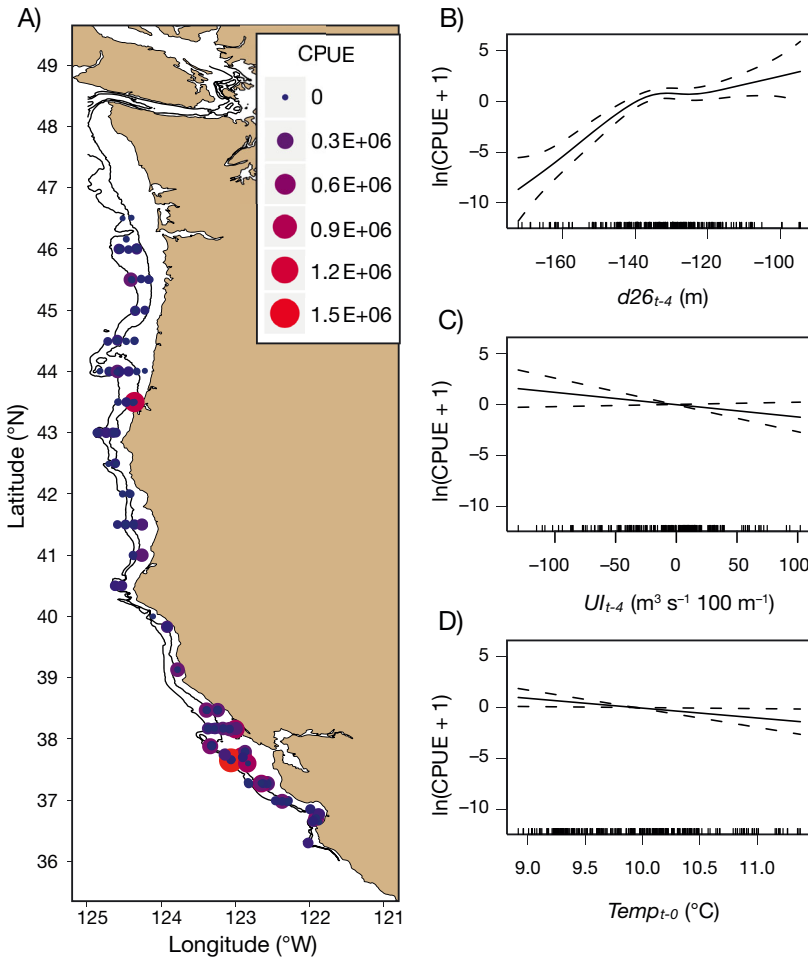


Fig. 5. (A) Krill abundance (catch per unit effort, CPUE) captured in each trawl (all 4 study years included). Also shown are the relationships between krill CPUE and (B) $Temp_{t-0}$, (C) $d26_{t-4}$, and (D) UI_{t-4} ; variables are defined in Table 2. Results in B–D are shown as partial responses based on the best generalized additive model (Model 1) in Table 4 (± 2 SE; dashed lines)

Table 4. Results for models of krill abundance variability along the shelf. Estimated degrees of freedom (edf) are listed next to each model covariate. Models 1–3 represent the best solutions after model selection among candidate models containing all possible combinations of the 5 environmental variables (plus the random effects *Station-Year*, and *Year*) used in our analyses. Model 4 (not supported) includes *Year* as a random effect in addition to the terms in Model 1. Variables are defined in Table 2. CPUE: catch per unit effort; re: random effects; * $p < 0.05$

Model	Krill ~ environmental models	R ² adj	Dev. expl (%)	ΔAIC	Significance of smooth terms (p)						
					$d26_{t-4}$	UI_{t-4}	$Temp_{t-0}$	U_{t-0}			
1	$\ln(\text{Krill CPUE} + 1) \sim s_1(d26_{t-4}) + s_2(UI_{t-4}) + s_3(Temp_{t-0}) + s_4(\text{Station-Year, re})$	0.413	55.50		<0.001*	3.7	0.09	1	0.03*	1	-
2	$\ln(\text{Krill CPUE} + 1) \sim s_1(d26_{t-4}) + s_2(Temp_{t-0}) + s_3(\text{Station-Year, re})$	0.410	55.40	1.12	<0.001*	3.3	-	-	0.07	1	-
3	$\ln(\text{Krill CPUE} + 1) \sim s_1(d26_{t-4}) + s_2(UI_{t-4}) + s_3(Temp_{t-0}) + s_4(U_{t-0}) + s_5(\text{Station-Year, re})$	0.410	55.30	1.87	<0.001*	3.7	0.09	1	0.03*	1	0.73
4	$\ln(\text{Krill CPUE} + 1) \sim s_1(d26_{t-4}) + s_2(UI_{t-4}) + s_3(Temp_{t-0}) + s_4(\text{Station-Year, re}) + s_5(\text{Year, re})$	0.410	54.80	5.31	<0.001*	3.7	0.32	1	0.08	1	-

sampling (U_{t-0}). The top model (Model 1, Table 4) included temperature during sampling ($Temp_{t-0}$) as well as winter upwelling (UI_{t-4}) and depth of the 26.0 kg m^{-3} isopycnal 4 mo prior ($d26_{t-4}$) (R^2 -adj = 0.41, deviance explained = 55.5%; Fig. 5B–D, Table 4). The depth of the 26.0 kg m^{-3} isopycnal 4 mo prior was the explanatory variable that was most strongly related to krill abundance in spring (Fig. 5C, Table 4). Increased krill abundance in spring was associated with a shallower 26.0 kg m^{-3} isopycnal in late winter, with an asymptote at 135 m. We did not see an effect of year in the krill model (Table 4).

DISCUSSION

We examined geographic and environmental determinants of juvenile salmon forage assemblages and found evidence of biogeographic provinces associated with capes and a latitudinal gradient associated with patterns of winter upwelling conditions. Market squid, rockfishes, and sanddabs were more dominant members of central CCE samples, and Pacific sand lance was more dominant in the northern CCE (Table 1). Importantly, we assessed environmental factors that relate to the regional abundance of forage species (e.g. winter preconditioning), as well as factors that impact spring-time spatial distribution of forage assemblages. Our findings indicate that distributions of salmon forage assemblages and the oceanographic characteristics associated with those assemblages are similar to the spatial coherence of salmon population survival observed over longer time series in the north-east Pacific Ocean (Mueter et al. 2002, Kilduff et al. 2014). Specifically, upwelling, forage assemblage, and survival dynamics vary at a scale of approximately 500–700 km along the CCE (Mueter et al. 2002, Kilduff et al. 2014), likely the result of winter downwelling north of Capes Mendocino and Blanco and upwelling south of these capes. Therefore, it is likely that ecosystem shifts leading to variation in the forage base in the north will affect salmon survival differently in the northern CCE than in the central CCE. We note, however, that coast-wide coherence of salmon survival may be increasing as a result of variability at the larger scale of the Pacific basin (Kilduff et al. 2015) and proximately by increasing coherence of forage assemblage dynamics along the CCE similar to the pattern observed in 2013 (Sakuma et al. 2016). In our results, this is indicated by the occurrence of the typically southern A4 assemblage in northern coastal waters (Fig. 4N).

We found that upwelling and winter preconditioning dynamics were the dominant determinants of assemblage differences along the CCE (Fig. 3). Two of the 4 assemblages we identified were consistently observed north of Cape Mendocino (assemblages 1 and 2) in association with downwelling, typical of the northern region in winter. Spring-time temperature was important for splitting closely distributed assemblages in the northern CCE. We also identified a central CCE assemblage (assemblage 4) that was predominantly distributed south of Cape Blanco and associated with winter upwelling. However, in 2013, assemblage 4 was also identified in the northern CCE, coincident with a period of atypically weak winter downwelling for that region. Additionally, in 2013, we identified a unique assemblage that occurred between the capes associated with an unusually shallow 26.0 kg m^{-3} isopycnal (assemblage 3, Fig. 4J). In 2013, the region between the capes had typical winter upwelling, making it distinct from the area to the north where downwelling was dramatically reduced and upwelling events occurred (Fig. 4N, Wells et al. 2013). Therefore, the association of assemblage type 3 with a shallow 26.0 kg m^{-3} isopycnal likely resulted from relatively strong southward transport through the region concomitant with the reduced downwelling and occasional upwelling in the north.

Biogeographic boundaries and mesoscale variability

The region between Capes Blanco and Mendocino represents a biogeographic break in the northern-central CCE for a number of marine taxa (Checkley & Barth 2009, Fenberg et al. 2015, Gottscho 2016). We observed a split in salmon forage assemblages in the same region, largely explained by differences in the timing, intensity, and structure of upwelling (Bograd et al. 2009, Checkley & Barth 2009). The region between Capes Blanco and Mendocino is characterized by a narrow shelf and had the greatest interannual variability of upwelling intensity along the CCE during the study period (Fig. 4) and, as a result, was characterized by variable turbulence and offshore and alongshore advection (Hickey 1979). North of Cape Blanco, the shelf is substantially wider and the coastline is oriented in a north–south direction (i.e. dominant current direction). South of Cape Mendocino the shelf narrows, coastal prominences are more common, and the dominant wind direction is north-east–southwest in the spring and summer. These

aspects of geography result in laminar upwelling north of Cape Blanco and meandering upwelling jets in central California (Strub et al. 1991). In the central region of the CCE, upwelling occurs throughout the year but typically strengthens in March to become especially strong in the summer. However, in the northern CCE, downwelling transitions to upwelling approximately in April, and the upwelling in the summer is weaker than in the central CCE (Bograd et al. 2009).

In addition to the broader regional differences between forage assemblage types north and south of the capes, mesoscale divisions between forage assemblages were also present. Specifically, assemblage type 1 (Figs. 3 & 4A–D) was associated with warmer temperatures than assemblage 2 (Figs. 3 & 4E–H). The spatial scale at which these assemblages differed was relatively fine (Fig. 4A–H), especially in 2014 and 2015. This suggests that modest behavioral differences and shifts in distribution of salmon could result in experiencing different forage assemblages. In this case, the assemblage associated with cooler water masses (assemblage 2) had higher ranks of market squid and rockfishes, both common salmon prey items in the region (see citations in Table 1), suggesting it may be a preferred forage assemblage for juvenile salmon. Similar mesoscale differences existed in 2013, during which an assemblage type was restricted between the capes and was distinct from the more dominant assemblage types occurring along the CCE (assemblage 3, Fig. 4J). This assemblage was characterized by higher-ranked abundances of Pacific hake relative to the northern assemblages and higher-ranked abundances of arrowtooth flounder relative to the northern and southern assemblage types (Table 1). YOY Pacific hake and arrowtooth flounder are typically observed farther offshore, but a shallow 26.0 kg m⁻³ isopycnal, such as that associated with this assemblage (Fig. 4J), is indicative of less on-shore transport to the region and increased alongshore transport through the region (Schroeder et al. 2014). The shelf in this region is very narrow such that off-shore derived taxa may simply be more common; as well, the relative abundance we observed may have been inflated by a reduction in the total number species observed. This locally distributed assemblage represented the fewest taxa, and a number of important salmon forage taxa were absent, including northern anchovy, Pacific sardine, and Pacific sand lance, likely as a result of advection from the region indicated by the exceptionally shallow 26.0 kg m⁻³ isopycnal (Schroeder et al. 2014).

Spatiotemporal variability of salmon forage assemblages

During our short study period, winter upwelling characteristics in the central CCE were largely asynchronous with the northern region (Fig. 4) and concomitant with that were distinct assemblage differences in the central and northern CCE. While 2015 had negative or neutral winter upwelling values in the central CCE (Fig. 4D,P), the difference between the northern and central CCE upwelling dynamics was sufficient to sustain distinct northern and southern assemblages (Fig. 4D,H,L,P). This suggests that relatively modest winter upwelling in the central CCE is capable of separating assemblages north and south of the capes. The most synchronous winter upwelling conditions along the CCE were in 2013, during which winter upwelling was intense south of Cape Blanco and downwelling was dramatically reduced north of Cape Blanco (i.e. conditions in the north were more similar to a typical winter in the central CCE). Perhaps as a result, the central CCE assemblage associated with winter upwelling was observed south and north of the capes, although represented by only 4 trawls in the north. Associated with reduced downwelling in the north in 2013 was a relatively shallow 26.0 kg m⁻³ isopycnal between the capes that resulted in a unique assemblage with few taxa (Fig. 4J). We argue that this likely resulted from advection of nearshore fishes from the narrow shelf of the region due to stronger than typical southward transport. Interestingly, across years the region between the capes was occupied by all assemblage types we observed. However, during any given year, the region was largely occupied by a single assemblage, suggesting the assemblage composition at this location is determined by the conditions north or south of it.

For an ecosystem characterized by high seasonal, interannual, and interdecadal variability, 4 years of data are not likely to have captured all of the possible states of this system. This is particularly true as these years have tended to be years of high variability in productivity for some species, such as YOY rockfishes, YOY sanddabs, and market squid, while reflecting very low abundance levels for other key prey, such as northern anchovy and Pacific sardine (McClatchie et al. 2016, Sakuma et al. 2016). The 2014–2015 period was one of highly anomalous atmospheric and ocean conditions throughout the northeastern Pacific, which has been referred to as a ‘marine heatwave,’ that was associated with unprecedented toxic algal blooms, fisheries closures,

widespread species range shifts, and unusual mortality events for several populations of seabirds and marine mammals (Leising et al. 2015, Cavole et al. 2016, DiLorenzo & Mantua 2016, Jacox et al. 2016, Santora et al. 2017). Across the CCE in 2015 there were increases in rockfish abundances, but there were decreases in krill abundance (Leising et al. 2015). Consistent with Schroeder et al. (2014), we show that krill abundance was negatively related to the depth of the 26.0 kg m⁻³ isopycnal (Fig. 5C).

We noted direct effects of the large marine heat-wave in 2015 on distributions of salmon forage assemblages on the shelf. The environmental signal is indicated by the exceptionally warm surface conditions off-shore in the northern CCE that is evident in Fig. 4H. The warm water mass in 2015 overlapped the shelf at a small area in the north (45–46°N; Fig. 4H). At the location where it did encroach on the shelf (Fig. 4D), our analysis shows the presence of assemblage 1 (our northern warm-water assemblage). During the same period, cooler waters impinged on the shelf in the north (Fig. 4H) and, associated with the band of cooler water, was the second northern assemblage. Despite limited samples, this indicates that divisions between the 2 distinct northern assemblages correspond to adjacent water masses.

A salmon perspective of forage assemblages

Within the CCE, juvenile salmon diets reflect the forage assemblages that we quantified (Brodeur et al. 2007, Wells et al. 2012, Hertz et al. 2015, Daly et al. 2017). Representative of regional forage availability, rockfishes and krill make up approximately half the diet of Chinook salmon by volume in the central CCE, while smelt and Pacific sand lance are significant forage taxa in the northern CCE (Hertz et al. 2015, Daly et al. 2017). Importantly, juvenile salmon diets covary with the spatiotemporal dynamics of the forage assemblages we quantified. For example, in 2011, when assemblage type 1, which contains Pacific sand lance, encompassed the northern region, Pacific sand lance was a significant contributor to the salmon diet (Daly et al. 2017). However, in 2015, during which assemblage type 2 impinged inshore of assemblage type 1 (Fig. 4D,H), Pacific sand lance were absent from the salmon diet (Daly et al. 2017). While assemblage type 2 does not contain Pacific sand lance, rockfishes are its most highly ranked taxon (Table 1). Concomitant with the presence of assemblage type 2 nearshore, rockfishes were the

dominant contributor to the salmon diet in 2015 (Daly et al. 2017). Importantly, these results support covariability between regional forage dynamics and diet, but they also demonstrate that meso-scale patterns between assemblage types 1 and 2 can determine the diet, and perhaps foraging behavior, of the salmon.

Broader implications for salmon dynamics and management

Although linking variability of forage communities directly to salmon survival is complicated and largely untestable here given our short time series, our results do provide a basis for exploring these relationships, as availability of the appropriate abundance and distribution of salmon forage is widely acknowledged to be a key factor in determining subsequent ocean survival. Importantly, we demonstrate that the distribution of forage assemblages could be the proximate driver of the spatial patterns of covariability between population survival dynamics revealed by Kilduff et al. (2014). However, the abundance and structure of forage assemblages available only tells part of the story. Salmon may be dependent upon the availability of lipid-rich prey to achieve high growth rates when they first enter the ocean. Previous studies have observed substantial seasonal and interannual variation in lipid and fatty acid profiles in both fish and invertebrates (Daly et al. 2010, Litz et al. 2010), which may be linked to bottom-up processes starting with the lower trophic levels (Litz et al. 2010, Miller et al. 2017). Therefore, the presence of a high abundance of young fish may not relate to strong recruitment if the fish are not the best for salmon energetically (Daly et al. 2013, 2017).

The specific structure of the salmon forage assemblage may have significant indirect effects on salmon survival as well. For instance, changes in the forage assemblage, as they relate to environmental drivers, can lead to changes in the foraging behavior of salmon predators (Emmett et al. 2006, Wells et al. 2017). Therefore, while we focus on the possibility of bottom-up drivers leading to variability in the forage base, such variability can affect the relative impact of predators on salmon as well. While Wells et al. (2017) focused on temporal variability in a given location (i.e. the central CCE), it is reasonable to extend those results and suggest that geographically distinct forage communities may determine, in part, the relative impact of predation on salmon along the CCE. For instance, juvenile salmon contribute 6–10% of the

common murre *Uria aalge* diet near the coast in Washington in the northern CCE (Schrimpf et al. 2012) and 9% in the Gulf of the Farallones in the central CCE, with increasing predation on salmon in years of low forage availability. The results we present here allow a first step toward developing a mechanistic understanding of bottom-up dynamics determining forage assemblages along the CCE. These considerations could, in turn, inform spatially explicit ecosystem models characterizing the dynamics between salmon and salmon predators.

Acknowledgements. This paper is a result of research supported by the National Oceanic and Atmospheric Administration's Integrated Ecosystem Assessment (NOAA IEA) Program. This paper is NOAA IEA program contribution #2018_6. Funding was provided by California Current Integrated Ecosystem Assessment and NOAA Fisheries. E. Daly, M. Henderson, and N. Mantua provided valuable advice. We thank the anonymous reviewers for their constructive feedback.

LITERATURE CITED

- Bakun A (1973) Coastal upwelling indices, West Coast of North America, 1946–71. NOAA Tech Rep NMFS SSRF-671. US Department of Commerce, NOAA, NMFS, Seattle, WA
- Bakun A, Parrish RH (1982) Turbulence, transport, and pelagic fish in the California and Peru Current systems. Calif Coop Ocean Fish Invest Rep 23:99–112
- ✦ Bakun A, Parrish RH (1990) Comparative studies of coastal pelagic fish reproductive habitats — the Brazilian sardine (*Sardinella aurita*). ICES J Mar Sci 46:269–283
- ✦ Beamish RJ, Mahnken C (2001) A critical size and period hypothesis to explain natural regulation of salmon abundance and the linkage to climate and climate change. Prog Oceanogr 49:423–435
- ✦ Bi H, Peterson WT, Lamb J, Casillas E (2011) Copepods and salmon: characterizing the spatial distribution of juvenile salmon along the Washington and Oregon coast, USA. Fish Oceanogr 20:125–138
- Bjorkstedt E, Goericke R, McClatchie S, Weber E and others (2012) State of the California Current 2010–2011: regional variable responses to a strong (but fleeting?) La Niña. Calif Coop Ocean Fish Invest Rep 52:36–68
- ✦ Black BA, Schroeder ID, Sydeman WJ, Bograd SJ, Wells BK, Schwing FB (2011) Winter and summer upwelling modes and their biological importance in the California Current Ecosystem. Glob Change Biol 17:2536–2545
- ✦ Bograd SJ, Schroeder I, Sarkar N, Qiu X, Sydeman WJ, Schwing FB (2009) Phenology of coastal upwelling in the California Current. Geophys Res Lett 36:L01602
- ✦ Bray JR, Curtis JT (1957) An ordination of upland forest communities of southern Wisconsin. Ecol Monogr 27: 325–349
- Breiman L, Friedman JH, Olshen RA, Stone CI (1984) Classification and regression trees. Wadsworth, Belmont, CA
- ✦ Brodeur RD (1989) Neustonic feeding by juvenile salmonids in coastal waters of the Northeast Pacific. Can J Zool 67: 1995–2007
- Brodeur RD, Pearcy WG (1990) Trophic relations of juvenile Pacific salmon off the Oregon and Washington Coast. Fish Bull 88:617–636
- ✦ Brodeur RD, Pearcy WG (1992) Effects of environmental variability on trophic interactions and food web structure in a pelagic upwelling ecosystem. Mar Ecol Prog Ser 84: 101–119
- ✦ Brodeur RD, Francis RC, Pearcy WG (1992) Food consumption of juvenile coho (*Oncorhynchus kisutch*) and chinook salmon (*O. tshawytscha*) on the continental shelf off Washington and Oregon. Can J Fish Aquat Sci 49:1670–1685
- Brodeur RD, Daly EA, Sturdevant MV, Miller TW and others (2007) Regional comparisons of juvenile salmon feeding in coastal marine waters off the west coast of North America. Am Fish Soc Symp 57:183–203
- ✦ Brodeur RD, Daly EA, Benkwitt CE, Morgan CA, Emmett RL (2011) Catching the prey: sampling juvenile fish and invertebrate prey fields of juvenile coho and Chinook salmon during their early marine residence. Fish Res 108:65–73
- Burnham KP, Anderson DR (2003) Model selection and multimodel inference: a practical information-theoretic approach. Springer Science & Business Media, New York, NY
- ✦ Cavole LM, Demko AM, Diner RE, Giddings A and others (2016) Biological impacts of the 2013–2015 warm-water anomaly in the Northeast Pacific: winners, losers, and the future. Oceanography 29:273–285
- Chambers JM, Cleveland WS, Kleiner B, Tukey PA (1983) Graphical methods for data analysis. Wadsworth, Belmont, CA
- ✦ Checkley DM, Barth JA (2009) Patterns and processes in the California Current System. Prog Oceanogr 83:49–64
- ✦ Cury P, Roy C (1989) Optimal environmental window and pelagic fish recruitment success in upwelling areas. Can J Fish Aquat Sci 46:670–680
- ✦ Daly EA, Brodeur RD, Weitkamp LA (2009) Ontogenetic shifts in diets of juvenile and subadult coho and Chinook salmon in coastal marine waters: important for marine survival? Trans Am Fish Soc 138:1420–1438
- ✦ Daly EA, Benkwitt CE, Brodeur RD, Litz MNC, Copeman LA (2010) Fatty acid profiles of juvenile salmon indicate prey selection strategies in coastal marine waters. Mar Biol 157:1975–1987
- ✦ Daly EA, Auth TD, Brodeur RD, Peterson WT (2013) Winter ichthyoplankton biomass as a predictor of early summer prey fields and survival of juvenile salmon in the northern California Current. Mar Ecol Prog Ser 484:203–217
- ✦ Daly EA, Brodeur RD, Auth TD (2017) Anomalous ocean conditions in 2015: impacts on spring Chinook salmon and their prey field. Mar Ecol Prog Ser 566:169–182
- ✦ De'ath G, Fabricius KE (2000) Classification and regression trees: a powerful yet simple technique for ecological data analysis. Ecology 81:3178–3192
- ✦ Di Lorenzo E, Mantua N (2016) Multi-year persistence of the 2014/15 North Pacific marine heatwave. Nat Clim Chang 6:1042–1047
- ✦ Di Lorenzo E, Schneider N, Cobb KM, Franks PJS and others (2008) North Pacific Gyre Oscillation links ocean climate and ecosystem change. Geophys Res Lett 35:L08607
- ✦ Dorman JG, Powell TM, Sydeman WJ, Bograd SJ (2011) Advection and starvation cause krill (*Euphausia pacifica*) decreases in 2005 Northern California coastal populations: implications from a model study. Geophys Res Lett 38:L04605
- ✦ Dorman JG, Sydeman WJ, García-Reyes M, Zeno RA, Santora JA (2015) Modeling krill aggregations in the central-northern California Current. Mar Ecol Prog Ser 528:87–99

- ✦ Dormann CF, Elith J, Bacher S, Buchmann C and others (2013) Collinearity: a review of methods to deal with it and a simulation study evaluating their performance. *Ecography* 36:27–46
- ✦ Emmett RL, Krutzikowsky GK, Bentley P (2006) Abundance and distribution of pelagic piscivorous fishes in the Columbia River plume during spring/early summer 1998–2003: relationship to oceanographic conditions, forage fishes, and juvenile salmonids. *Prog Oceanogr* 68: 1–26
- ✦ Fenberg PB, Menge BA, Raimondi PT, Rivadeneira MM (2015) Biogeographic structure of the northeastern Pacific rocky intertidal: the role of upwelling and dispersal to drive patterns. *Ecography* 38:83–95
- ✦ Fiechter J, Huff DD, Martin BT, Jackson DW and others (2015) Environmental conditions impacting juvenile Chinook salmon growth off central California: an ecosystem model analysis. *Geophys Res Lett* 42:2910–2917
- ✦ Garcia-Reyes M, Largier JL, Sydeman WJ (2014) Synoptic-scale upwelling indices and predictions of phyto- and zooplankton populations. *Prog Oceanogr* 120:177–188
- ✦ Gottscho AD (2016) Zoogeography of the San Andreas Fault system: Great Pacific Fracture Zones correspond with spatially concordant phylogeographic boundaries in western North America. *Biol Rev Camb Philos Soc* 91: 235–254
- ✦ Hassrick JL, Henderson MJ, Huff DD, Sydeman WJ and others (2016) Early ocean distribution of juvenile Chinook salmon in an upwelling ecosystem. *Fish Oceanogr* 25: 133–146
- ✦ Hertz E, Trudel M, Brodeur RD, Daly EA and others (2015) Continental-scale variability in the feeding ecology of juvenile Chinook salmon along the coastal Northeast Pacific Ocean. *Mar Ecol Prog Ser* 537:247–263
- ✦ Hickey BM (1979) The California Current System—hypotheses and facts. *Prog Oceanogr* 8:191–279
- ✦ Jacox MG, Fiechter J, Moore AM, Edwards CA (2015) ENSO and the California Current coastal upwelling response. *J Geophys Res Oceans* 120:1691–1702
- ✦ Jacox MG, Hazen EL, Zaba KD, Rudnick DL, Edwards CA, Moore AM, Bograd SJ (2016) Impacts of the 2015–2016 El Niño on the California Current System: early assessment and comparison to past events. *Geophys Res Lett* 43:7072–7080
- Jones E, Oliphant T, Peterson P (2001) SciPy: Open source scientific tools for Python. www.scipy.org/
- ✦ Kaplan IC, Brown CJ, Fulton EA, Gray IA, Field JC, Smith AD (2013) Impacts of depleting forage species in the California Current. *Environ Conserv* 40:380–393
- ✦ Kilduff DP, Botsford LW, Teo SLH (2014) Spatial and temporal covariability in early ocean survival of Chinook salmon (*Oncorhynchus tshawytscha*) along the west coast of North America. *ICES J Mar Sci* 71:1671–1682
- ✦ Kilduff DP, Di Lorenzo E, Botsford LW, Teo SLH (2015) Changing central Pacific El Niños reduce stability of North American salmon survival rates. *Proc Natl Acad Sci USA* 112:10962–10966
- ✦ King JR, Agostini VN, Harvey CJ, McFarlane GA and others (2011) Climate forcing and the California Current ecosystem. *ICES J Mar Sci* 68:1199–1216
- ✦ Koehn LE, Essington TE, Marshall KN, Kaplan IC, Sydeman WJ, Szoboszlai AI, Thayer JA (2016) Developing a high taxonomic resolution food web model to assess the functional role of forage fish in the California Current ecosystem. *Ecol Model* 335:87–100
- ✦ Largier JL, Lawrence CA, Roughan M, Kaplan DM and others (2006) WEST: a northern California study of the role of wind-driven transport in the productivity of coastal plankton communities. *Deep Sea Res II* 53:2833–2849
- Leising AW, Schroeder ID, Bograd SJ, Bjorkstedt EP and others (2014) State of the California Current 2013–14: El Niño looming. *Calif Coop Ocean Fish Invest Rep* 55:51–87
- Leising AW, Schroeder ID, Bograd SJ, Abell J and others (2015) State of the California Current 2014–15: impacts of the warm-water ‘blob’. *Calif Coop Ocean Fish Invest Rep* 56:31–68
- ✦ Litz MNC, Brodeur RD, Emmett RL, Heppell SS, Rasmussen RS, O’Higgins L, Morris MS (2010) Effects of variable oceanographic conditions on forage fish lipid content and fatty acid composition in the northern California Current. *Mar Ecol Prog Ser* 405:71–85
- ✦ Logerwell EA, Mantua N, Lawson PW, Francis RC, Agostini VN (2003) Tracking environmental processes in the coastal zone for understanding and predicting Oregon coho (*Oncorhynchus kisutch*) marine survival. *Fish Oceanogr* 12:554–568
- ✦ Loh WY (2011) Classification and regression trees. *Wiley Interdiscip Rev Data Min Knowl Discov* 1:14–23
- ✦ MacFarlane RB (2010) Energy dynamics and growth of Chinook salmon (*Oncorhynchus tshawytscha*) from the Central Valley of California during the estuarine phase and first ocean year. *Can J Fish Aquat Sci* 67:1549–1565
- MacFarlane RB, Norton EC (2002) Physiological ecology of juvenile chinook salmon (*Oncorhynchus tshawytscha*) at the southern end of their distribution, the San Francisco Estuary and Gulf of the Farallones, California. *Fish Bull* 100:244–257
- ✦ Mantua NJ, Hare SR, Zhang Y, Wallace JM, Francis RC (1997) A Pacific interdecadal climate oscillation with impacts on salmon production. *Bull Am Meteorol Soc* 78: 1069–1079
- McClatchie S, Goericke R, Leising A, Auth TD and others (2016) State of the California Current 2015–16: comparisons with the 1997–98 El Niño. *Calif Coop Ocean Fish Invest Rep* 57:5–61
- McCune B, Grace JB, Urban DL (2002) Analysis of ecological communities (Vol 28). MjM software design, Glendeden Beach, OR
- ✦ Miller JA, Peterson WT, Copeman LA, Du X, Morgan CA, Litz MNC (2017) Temporal variation in the biochemical ecology of lower trophic levels in the Northern California Current. *Prog Oceanogr* 155:1–12
- ✦ Moore AM, Arango HG, Broquet G, Powell BS, Weaver AT, Zavala-Garay J (2011) The Regional Ocean Modeling System (ROMS) 4-dimensional variational data assimilation systems. Part I—System overview and formulation. *Prog Oceanogr* 91:34–49
- ✦ Mueter FJ, Ware DM, Peterman RM (2002) Spatial correlation patterns in coastal environmental variables and survival rates of salmon in the north-east Pacific Ocean. *Fish Oceanogr* 11:205–218
- Oksanen J, Blanchet FG, Friendly M, Kindt R and others (2016) Vegan: community ecology package. R package version 2.4-1. <https://CRAN.R-project.org/package=vegan>
- Pacific Fisheries Management Council (2013) Pacific Coast fishery ecosystem plan for the U.S. portion of the California Current Large Marine Ecosystem. Pacific Fishery Management Council, Portland, OR
- Parrish RH, Nelson CS, Bakun A (1981) Transport mechanisms and reproductive success of fishes in the California Current. *Biol Oceanogr* 1:175–203
- ✦ Phillips AJ, Brodeur RD, Sunstov AV (2009) Micronekton community structure in the epipelagic zone of the northern California Current upwelling system. *Prog Oceanogr* 80:74–92

- R Core Team (2015) R: a language and environment for statistical computing. R Foundation for Statistical Computing, Vienna
- ✦ Ralston S, Sakuma KM, Field JC (2013) Interannual variation in pelagic juvenile rockfish (*Sebastes* spp.) abundance—going with the flow. *Fish Oceanogr* 22:288–308
- ✦ Ralston S, Field JC, Sakuma KM (2015) Long-term variation in a central California pelagic forage assemblage. *J Mar Syst* 146:26–37
- Riddell B, Brodeur RD, Bugaev AV, Moran P and others (2018) Ocean ecology of Chinook salmon. In: Beamish RJ (ed.) *The ocean ecology of salmon and trout*. American Fisheries Society, Bethesda, MD, p 555–696
- ✦ Ruzicka JJ, Brodeur RD, Emmett RL, Steele JH and others (2012) Interannual variability in the Northern California Current food web structure: changes in energy flow pathways and the role of forage fish, euphausiids, and jellyfish. *Prog Oceanogr* 102:19–41
- Sakamoto Y, Ishiguro M, Kitagawa G (1986) Akaike information criterion statistics. D. Reidel Publishing Company, Dordrecht
- Sakuma KM, Field JC, Mantua NJ, Ralston S, Marinovic BB, Carrion CN (2016) Anomalous epipelagic micronekton assemblage patterns in the neritic waters of the California Current in spring 2015 during a period of extreme ocean conditions. *Calif Coop Ocean Fish Invest Rep* 57: 163–183
- ✦ Santora JA, Sydeman WJ, Schroeder ID, Wells BK, Field JC (2011) Mesoscale structure and oceanographic determinants of krill hotspots in the California Current: implications for trophic transfer and conservation. *Prog Oceanogr* 91:397–409
- ✦ Santora JA, Field JC, Schroeder ID, Sakuma KM, Wells BK, Sydeman WJ (2012a) Spatial ecology of krill, micronekton and top predators in the central California Current: implications for defining ecologically important areas. *Prog Oceanogr* 106:154–174
- ✦ Santora JA, Sydeman WJ, Schroeder ID, Reiss CS and others (2012b) Krill space: a comparative assessment of mesoscale structuring in polar and temperate marine ecosystems. *ICES J Mar Sci* 69:1317–1327
- ✦ Santora JA, Hazen EL, Schroeder ID, Bograd SJ, Sakuma KM, Field JC (2017) Impacts of ocean climate variability on biodiversity of pelagic forage species in an upwelling ecosystem. *Mar Ecol Prog Ser* 580:205–220
- ✦ Satterthwaite WH, Carlson SM, Allen-Moran SD, Vincenzi S, Bograd SJ, Wells BK (2014) Match-mismatch dynamics and the relationship between ocean-entry timing and relative ocean recoveries of Central Valley fall run Chinook salmon. *Mar Ecol Prog Ser* 511:237–248
- ✦ Schabetsberger R, Morgan CA, Brodeur RD, Potts CL, Peterson WT, Emmett RL (2003) Prey selectivity and diel feeding chronology of juvenile chinook (*Oncorhynchus tshawytscha*) and coho (*O. kisutch*) salmon in the Columbia River plume. *Fish Oceanogr* 12:523–540
- ✦ Schrimpf MB, Parrish JK, Pearson SF (2012) Trade-offs in prey quality and quantity revealed through the behavioral compensation of breeding seabirds. *Mar Ecol Prog Ser* 460:247–259
- ✦ Schroeder ID, Sydeman WJ, Sarkar N, Thompson SA, Bograd SJ, Schwing FB (2009) Winter pre-conditioning of seabird phenology in the California Current. *Mar Ecol Prog Ser* 393:211–223
- ✦ Schroeder ID, Black BA, Sydeman WJ, Bograd SJ, Hazen EL, Santora JA, Wells BK (2013) The North Pacific High and wintertime pre-conditioning of California Current productivity. *Geophys Res Lett* 40:541–546
- ✦ Schroeder ID, Santora JA, Moore AM, Edwards CA and others (2014) Application of a data-assimilative regional ocean modeling system for assessing California Current System ocean conditions, krill, and juvenile rockfish interannual variability. *Geophys Res Lett* 41:5942–5950
- Schwing FB, O'Farrell M, Steger JM, Baltz K (1996) Coastal upwelling indices, West Coast of North America, 1946–1995. NOAA Tech Memo NOAA-TM-NMFS-SWFSC-231. US Department of Commerce, NOAA, NMFS, Pacific Grove, CA
- ✦ Strub PT, Kosro PM, Huyer A (1991) The nature of the cold filaments in the California Current System. *J Geophys Res* 96:14, 743–14, 768
- ✦ Thayer JA, Field JC, Sydeman WJ (2014) Changes in California Chinook salmon diet over the past 50 years: relevance to the recent population crash. *Mar Ecol Prog Ser* 498:249–261
- Therneau TM, Atkinson EJ (1997) An introduction to recursive partitioning using the RPART Routines. Tech Rep 61. Mayo Foundation. <http://www.mayo.edu/research/documents/biostat-61pdf/doc-10026699>
- Therneau TM, Atkinson EJ (2018) An introduction to recursive partitioning using the RPART Routines. Mayo Foundation. <https://cran.r-project.org/web/packages/rpart/vignettes/longintro.pdf>
- Therneau T, Anderson B, Ripley B (2015) Package 'rpart'. R package version 4.1-10. <https://cran.r-project.org/package/rpart>
- ✦ Tucker S, Hipfner JM, Trudel M (2016) Size- and condition-dependent predation: a seabird disproportionately targets substandard individual juvenile salmon. *Ecology* 97: 461–471
- ✦ Wells BK, Santora JA, Field JC, MacFarlane RB, Marinovic BB, Sydeman WJ (2012) Population dynamics of Chinook salmon *Oncorhynchus tshawytscha* relative to prey availability in the central California coastal region. *Mar Ecol Prog Ser* 457:125–137
- Wells BK, Schroeder ID, Santora JA, Hazen EL and others (2013) State of the California Current 2012–2013: no such thing as an 'average' year. *Calif Coop Ocean Fish Invest Rep* 54:37–71
- ✦ Wells BK, Santora JA, Schroeder ID, Mantua N, Sydeman WJ, Huff DD, Field JC (2016) Marine ecosystem perspectives on Chinook salmon recruitment: a synthesis of empirical and modeling studies from a California upwelling system. *Mar Ecol Prog Ser* 552:271–284
- ✦ Wells BK, Santora JA, Henderson MJ, Warzybok P and others (2017) Environmental conditions and prey-switching by a seabird predator impact juvenile salmon survival. *J Mar Syst* 174:54–63
- ✦ Wing SR, Botsford LW, Ralston SV, Largier JL (1998) Mero-planktonic distribution and circulation in a coastal retention zone of the northern California upwelling system. *Limnol Oceanogr* 43:1710–1721
- ✦ Wolter K, Timlin MS (1998) Measuring the strength of ENSO events—How does 1997/98 rank? *Weather* 53: 315–324
- Wood SN (2006) Generalized additive models: an introduction with R. Chapman and Hall/CRC, Boca Raton, FL
- ✦ Woodson CB, Litvin SY (2015) Ocean fronts drive marine fishery production and biogeochemical cycling. *Proc Natl Acad Sci USA* 112:1710–1715
- ✦ Woodson LE, Wells BK, Weber PK, MacFarlane RB, Whitman GE, Johnson RC (2013) Size, growth, and origin-dependent mortality of juvenile Chinook salmon *Oncorhynchus tshawytscha* during early ocean residence. *Mar Ecol Prog Ser* 487:163–175